MOLECULAR TOXICOLOGY

Identification of novel agonists by high-throughput screening and molecular modelling of human constitutive androstane receptor isoform 3

Oliver Keminer[1] · Björn Windshügel[1] · Frank Essmann[2,3] · Serene M. L. Lee[4] · Tobias S. Schiergens[4] · Matthias Schwab[2,5] · Oliver Burk[2,3]

Abstract

Prediction of drug interactions, based on the induction of drug disposition, calls for the identification of chemicals, which activate xenosensing nuclear receptors. Constitutive androstane receptor (CAR) is one of the major human xenosensors; however, the constitutive activity of its reference variant CAR1 in immortalized cell lines complicates the identification of agonists. The exclusively ligand-dependent isoform CAR3 represents an obvious alternative for screening of CAR agonists. As CAR3 is even more abundant in human liver than CAR1, identification of its agonists is also of pharmacological value in its own right. We here established a cellular high-throughput screening assay for CAR3 to identify ligands of this isoform and to analyse its suitability for identifying CAR ligands in general. Proof-of-concept screening of 2054 drug-like compounds at 10 μM resulted in the identification of novel CAR3 agonists. The CAR3 assay proved to detect the previously described CAR1 ligands in the screened libraries. However, we failed to detect CAR3-selective compounds, as the four novel agonists, which were selected for further investigations, all proved to activate CAR1 in different cellular and in vitro assays. In primary human hepatocytes, the compounds preferentially induced the expression of the prototypical CAR target gene CYP2B6. Failure to identify CAR3-selective compounds was investigated by molecular modelling, which showed that the isoform-specific insertion of five amino acids did not impact on the ligand binding pocket but only on heterodimerization with retinoid X receptor. In conclusion, we demonstrate here the usability of CAR3 for screening compound libraries for the presence of CAR agonists.

Oliver Keminer and Björn Windshügel contributed equally to this work.

✉ Björn Windshügel
bjoern.windshuegel@ime.fraunhofer.de

✉ Oliver Burk
oliver.burk@ikp-stuttgart.de

[1] Fraunhofer Institute for Molecular Biology and Applied Ecology IME, Schnackenburgallee 114, 22525 Hamburg, Germany

[2] Dr. Margarete Fischer-Bosch-Institute of Clinical Pharmacology, Auerbachstrasse 112, 70376 Stuttgart, Germany

[3] University of Tübingen, Tübingen, Germany

[4] Biobank of the Department of General, Visceral, and Transplant Surgery, Ludwig-Maximilians-University Munich, Munich, Germany

[5] Departments of Clinical Pharmacology, Pharmacy and Biochemistry, University of Tübingen, Tübingen, Germany

Introduction

The constitutive androstane receptor (CAR, NR1I3) primarily induces the transcription of genes involved in absorption, distribution, metabolism and excretion

(ADME) of xenobiotics. CAR binds as a heterodimer with retinoid X receptor (RXR) α to specific DNA response elements in the regulatory region of its target genes after being activated by small molecules. These either directly bind as ligands into the ligand-binding pocket (LBP), or indirectly promote translocation of the receptor into the nucleus (Yang and Wang 2014). CYP2B6 represents the prototypical CAR target gene; however, the receptor also regulates further genes of the cytochrome P450 superfamily (Kandel et al. 2016), as well as ABC efflux transporters (Burk et al. 2005a). By inducing ADME gene expression and subsequently accelerating drug detoxification, activation of CAR may affect the success of pharmacotherapy. In addition, CAR participates in the regulation of glucose and lipid metabolism and may thus be a potential novel therapeutic target for the treatment of metabolic diseases, such as obesity, type 2 diabetes and fatty liver, where energy metabolism is dysregulated (Jiang and Xie 2013). Thus, identifying CAR activators is not only of importance for predicting drug interactions and preventing drug failure or toxicity, but also for opening new avenues for the treatment of human diseases.

Identification of indirect activators requires establishing nuclear translocation assays in translocation-competent cells, as, e.g. primary hepatocytes. A respective high-content screening method was only recently developed (Mackowiak and Wang 2019). In contrast, direct activators, i.e. ligands, can more easily be screened using reporter gene assays. However, the constitutive transactivation activity of the reference isoform CAR1 and its constitutive nuclear localization in immortalized cell lines impedes their identification. Different strategies and cellular screening assays have been employed to overcome this obstacle. First, mammalian one-hybrid assays using fusion proteins of full-length CAR (Dring et al. 2010) or the CAR ligand binding domain (LBD) (Küblbeck et al. 2011) with the GAL4 DNA binding domain (DBD) have been applied to screen small compound sets for CAR activation. Ligand-dependency of the CAR-LBD fusion protein was further improved by inserting three consecutive alanine residues into the loop between helices H10/11 and H12 (Kanno and Inouye 2010). However, the foreign DBD may influence results, as structural studies of full-length nuclear receptor heterodimers have illustrated the importance of inter-domain interactions for the LBD conformation (Rastinejad et al. 2013). Second, a synthetic ligand-dependent CAR1 insertion mutant has been used to confirm activation by a small set of compounds, which were predicted in silico to bind to CAR (Lynch et al. 2013). However, the mutant has only been tested for equal performance with a very limited number of compounds (Chen et al. 2010). Third, prior deactivation of full-length CAR1 by an inverse agonist has been used to allow for high-throughput screening (HTS) of a library of drug-like compounds for

agonists (Lynch et al. 2015). Here, results may be limited by the choice of the inverse agonist.

Besides the constitutively active reference variant CAR1, a natural and exclusively ligand-dependent isoform, called CAR3 (Auerbach et al. 2005), CAR-SV2 (Arnold et al. 2004; Jinno et al. 2004) or CAR-SV24 (Lamba et al. 2005), has been described. It is generated by alternative splicing, which results in the in-frame insertion of five amino acids (APYLT) into the LBD (Auerbach et al. 2003). This insertion expands the loop connecting LBD helices α8 and α9. Homology modelling predicted sterical hindrance of the dimerization with RXRα (Auerbach et al. 2003). In contrast to CAR1, CAR3 shows exclusive ligand-dependent interaction with coactivators (Arnold et al. 2004), resulting in ligand-dependent transcriptional activity (Auerbach et al. 2005). CAR3, accounting for roughly 50% of total CAR transcripts, is on average even more abundant in human liver than the reference variant CAR1 (Jinno et al. 2004; Ross et al. 2010). Thus, the identification of compounds activating this isoform has its own pharmacological value.

Previously identified agonists of CAR3 comprise, among others, the prototypical human CAR1 agonist CITCO (Auerbach et al. 2005), bisphenol A (DeKeyser et al. 2011), artemisinin, arteether and artemether (Burk et al. 2012), as well as the CAR1 inverse agonists clotrimazole and NF49 (Anderson et al. 2011). In addition, three compounds, claimed to selectively activate CAR3, have been described (Dring et al. 2010). The existence of CAR3-selective compounds remains obscure, as a homology model indicated a virtually identical LBP volume and shape compared to the LBP in the CAR1 X-ray crystal structure (Omiecinski et al. 2011), suggesting that CAR1 and CAR3 should bind the same molecules.

Given the inherent limitations of previously used screening assays for CAR ligands, based on CAR1 or synthetic mutants thereof, and to identify novel CAR3 activators, we established a corresponding cellular HTS assay. Screening of two libraries of pharmacologically active compounds with altogether 2054 chemicals resulted in the identification of novel CAR3 agonists, which were further investigated using cellular, biochemical and in silico methods. Furthermore, we used molecular modelling and molecular dynamics simulations to study the impact of the five amino acid insertion in CAR3 on the LBP as well as on its interactions with RXRα.

Materials and methods

Materials

The SCREEN-WELL® FDA approved drug library V2 with 774 compounds and the Library of Pharmacologically Active Compounds (LOPAC®1280) with 1280 compounds

were purchased from Enzo Life Sciences (Lörrach, Germany) and Sigma-Aldrich (Munich, Germany), respectively. A detailed description of further chemical and biological reagents and of the plasmids, which have been used in this study, is provided in the electronic supplementary material.

Cell culture

HEK293T cells (ACC 635, DSMZ, Braunschweig, Germany) were grown in high glucose DMEM, supplemented with 10% FBS, 2 mM L-glutamine, 100 U/ml penicillin and 100 µg/ml streptomycin. HepG2 cells (HB-8065, lot number 58,341,723) were obtained from ATCC (Manassas, VA) at passage 74, propagated and used in transfection experiments between passages 90 and 120. Passage number of HepG2 cells did not impact on the results of reporter gene analyses. HepG2 cells were cultivated in minimal essential medium, supplemented with 10% FBS, 2 mM L-glutamine, 100 U/ml penicillin and 100 µg/ml streptomycin. During treatment with chemicals, regular FBS was replaced by dextran-coated charcoal-stripped FBS. Cells were routinely checked for contamination with mycoplasma by PCR (VenorGeM Classic, Minerva Biolabs, Berlin, Germany).

High-throughput screening and hit confirmation

HEK293T instead of HepG2 cells were selected for establishing the HTS assay, because they were easily and more efficiently transfected and better tolerated the automated cell seeding procedure, which was required to miniaturize the assay to the 384-well plate format (see below). Pilot experiments confirmed CITCO-dependent CAR3 activity in HEK293T cells. The cells were transfected in suspension using Effectene Transfection Reagent (Qiagen, Hilden, Germany), according to the recommendations of the manufacturer. Briefly, the required multitude of 13,000 cells/well (25 µl) were re-suspended in culture medium supplemented with 1% dextran-coated charcoal-stripped FBS. Cells were co-transfected with expression plasmids encoding human CAR3 and RXRα, CYP3A4 reporter plasmid and pRL-TK at the ratio of 1:1:15:5. A total of 12.5 ng DNA was transfected per well. The suspension of transfected cells was seeded in white 384-well plates (Greiner Bio-One, Frickenhausen, Germany) using a Multidrop™ 384 reagent dispenser (Thermo Fisher Scientific, Dreieich, Germany). After 16 h incubation, cells were either treated with DMSO (background control), 10 µM CITCO (positive control) or 10 µM of a library compound for additional 24 h. The DMSO concentration of all samples was adjusted to 0.625%. Compound transfer was carried out as described before (Burk et al. 2018). Cell lysates were assayed for firefly and *Renilla* luciferase activities, using the Dual-Glo® Luciferase Assay System, (Promega, Madison, WI), and EnVision

multilabel plate reader (PerkinElmer, Rodgau, Germany). Relative reporter activity was calculated by dividing the firefly luciferase by the *Renilla* luciferase activity measured in the same well. The respective activities of cells treated with chemicals were compared to the activity of cells in the background control, which was designated 1. Quality and robustness of HTS were evaluated as previously described (Burk et al. 2018), by calculating Z prime (Z′) according to Zhang et al. (1999). Plates were considered valid for further analyses if $Z' > 0.4$. To minimize the loss of weak activators and thus reducing false negatives, a threshold of ≥ twofold induction was defined for compounds to be regarded as hits. Hit confirmation was either done as dose response or replicate (10 µM, $N = 5$) analysis.

Transient transfection and reporter gene analysis

Transient co-transfections were carried out in 24-well plates with 1.5×10^5 HepG2 cells per well, seeded the day before, using per well 1 µl jetPRIME® transfection reagent (Polyplus, Illkirch, France) and a plasmid DNA mixture consisting of 0.3 µg of CYP2B6 reporter gene plasmid, 0.02 µg of human CAR3 and human RXRα expression plasmids each, 0.01 µg of pRL-CMV, filled up to 0.5 µg with pUC18. In some experiments, 0.04 µg of human CAR1 or PXR expression plasmids replaced the CAR3/RXRα combination. CAR or PXR expression plasmids were substituted by empty vector pcDNA3 in negative controls. Transfections for mammalian two-hybrid CAR1 coactivator recruitment and LBD assembly assays were done similarly, using the plasmids specified in the legends of Figs. 3a and 4. 20 h after transfection, cells were treated with the indicated chemicals for another 24 h. Then cells were lysed with 1× passive lysis buffer (Promega) and firefly and *Renilla* luciferase assays were done as described (Geick et al. 2001; Piedade et al. 2015). For normalization of reporter activity, the ratio of the corresponding firefly and *Renilla* luciferase activities was calculated. All transfections were done at least three times independently, each in technical triplicates.

Coactivator-dependent receptor ligand assay (CARLA)

Radiolabelled full-length CAR1 protein was synthesized in vitro using the respective expression plasmid, TNT T7 coupled transcription/translation system (Promega) and ^{35}S-methionine (specific activity > 1000 Ci/mmol, Hartmann Analytic, Braunschweig, Germany). The bacterially expressed fusion protein of NH_2–terminal glutathione S transferase (GST) moiety and receptor interaction domain (RID) of human SRC1 (amino acids 583–783) was prepared and CARLA essentially performed as described previously (Burk et al. 2012).

Primary human hepatocytes

Double-coded liver tissue used in this study was provided by the Biobank of the Department of General, Visceral and Transplant Surgery in Ludwig-Maximilians-University (LMU). This Biobank operates under the administration of the Human Tissue and Cell Research (HTCR) Foundation. The framework of HTCR Foundation (Thasler et al. 2003), which includes obtaining written informed consent from all donors, has been approved by the ethics commission of the Faculty of Medicine at the LMU (approval number 025-12) as well as the Bavarian State Medical Association (approval number 11142) in Germany. Primary human hepatocytes were isolated from liver tissue samples by the Biobank of the Department of General, Visceral and Transplant Surgery in LMU using a two-step collagenase perfusion technique with modifications (Lee et al. 2013). The cells were received at the laboratory in Stuttgart as suspensions on ice within 16–20 h after preparation and cultivated and treated with chemicals as described before (Jeske et al. 2017). Donor data are shown in Supplementary Table S1.

RNA isolation and reverse transcription quantitative real-time PCR analysis

Total RNA was prepared using the NucleoSpin RNA kit (Macherey–Nagel, Düren, Germany) combined with on-column DNase I digest to remove residual genomic DNA. RNA integrity was monitored using formaldehyde agarose gel electrophoresis. cDNA was synthesized as described previously (Jeske et al. 2017). Relative quantification of mRNA expression ($\Delta\Delta Ct$) was performed by TaqMan real-time PCR using the Biomark HD system and FlexSix Gene Expression Integrated Fluidic Circuits (Fluidigm, South San Francisco, CA) as described before (Bitter et al. 2015). The commercial TaqMan gene expression assays Hs00184500_m1 and Hs00604506_m1 (Life Technologies, Darmstadt, Germany) were used to quantify ABCB1 and CYP3A4, respectively. The CYP2B6 (Burk et al. 2005b) and 18S assays (Hoffart et al. 2012) have been described previously. Measurements were conducted in technical triplicates and data were analysed as described before (Jeske et al. 2017).

Molecular modelling

A homology model of the CAR3 LBD in complex with the RXRα LBD was constructed using the X-ray crystal structure of the CAR1/RXRα heterodimer (PDB ID 1XVP) as modelling template. Based on an assessment of the two CAR/RXRα complexes using PROCHECK and ProSa (Laskowski et al. 1993; Sippl 2007), chains C (RXRα) and D (CAR) were selected. The loop connecting α8 and α9 was modelled using SYBYL-X 1.2 (Certara, Princeton, NJ, USA). Missing side chains of the loop residues were placed using the software Molecular Operating Environment (MOE), version 2018.0101 (Chemical Computing Group Inc., Montreal, Canada).

Molecular dynamics simulations using the CAR1 X-ray crystal structure and the CAR3 homology model were prepared and carried out with the GROMACS 2018.2 software suite (www.gromacs.org). The Amber99SB-ILDN force field was selected (Lindorff-Larsen et al. 2010). Each protein was placed in a box filled with water molecules and Na^+ ions for charge neutralisation (CAR1: 16,352 water molecules, 4 ions; CAR3: 17,885, 4 ions). Water molecules placed within the protein interior were deleted, if the hydration free energy of the site, calculated using the 3D RISM method in MOE, was not negative. After 500 steps of energy minimization using the Steepest Descent method, each simulation system was equilibrated using three short (100 ps each) simulations (NVT and NPT ensemble), with gradually releasing atom position constraints (NVT: 1000 kcal/mol on all protein heavy atoms; NPT 1: 1000 kcal/mol on all protein heavy atoms; NPT 2: 1000 kcal/mol on protein backbone atoms). Initial velocities were taken from a Maxwell–Boltzmann distribution at 298 K. After equilibration, a 500 ns unconstrained simulation was carried out. Structures were saved every 10 ps. All bonds involving hydrogen atoms were constrained to their equilibrium values by means of the LINCS algorithm. Constant temperature (298 K) was maintained using a Nosé–Hoover thermostat (298 K, time constant $\tau = 1$ ps). In the NPT ensemble simulations, a constant pressure was maintained using the Parrinello–Rahman barostat (1 bar, $\tau = 2$ ps). The neighbour lists for non-bonded interactions were updated every ten steps. The long-ranged electrostatic interactions were calculated by the Particle-Mesh-Ewald method. The short-ranged van der Waals and electrostatic interactions were cut-off at 1 nm.

Pocket volume calculations of the MD simulations frames were done using MDpocket (Schmidtke et al. 2010).

Molecular docking

Molecular docking was carried out using GOLD version 5.7 (Cambridge Crystallographic Data Centre, Cambridge, UK) and the ChemPLP scoring function. Preparation of X-ray crystal structures and generation of ligand structures to be docked was conducted as described before (Jeske et al. 2017). For each compound 50 docking runs were carried out. Non-default docking parameters have been described previously (Jeske et al. 2017).

Data analyses

Data are presented as mean $\pm$ SD of three to eight independent experiments (see respective figure legends), with

the exception of Fig. 7 and Supplementary Fig. S6, where data of individual hepatocyte donors are shown separately as mean $\pm$ SD of technical triplicates. The order of chemical treatment of cells and measurement of samples was changed in independent experiments, to avoid systematic errors due to timing or positioning. Data were not transformed, but normalized to vehicle treatment or to vehicle-treated negative controls, to adjust for the experimental variability of raw values. Statistical analyses were done using ordinary or repeated measures one-way or two-way ANOVA, with post hoc tests for multiple comparisons against controls as recommended by the analysis software and described in the respective figure legends. EC_{50} determinations were done by nonlinear fit of dose response using the equation for sigmoidal dose response with variable slope, and bottom values fixed to 1. All calculations were done with GraphPad Prism 8.1.1 (GraphPad software, La Jolla, CA, USA).

Results

Identification of novel CAR3 agonists

A HTS assay for the identification of CAR3 activators was set up in the 384-well plate format with HEK293T cells and the CYP3A4 reporter. As it was previously described that CAR3-dependent induction of cytochrome P450 enhancer/promoter-based reporter gene activity strictly depends on RXRα overexpression (Auerbach et al. 2005), a respective expression plasmid was co-transfected. Treatment with positive control CITCO resulted in mean 26.7 ± 3.3-fold induction as compared to treatment with vehicle DMSO only. Altogether, 2054 compounds, consisting of the 774 compounds of the SCREEN-WELL® FDA approved drug library V2 and the 1280 compounds of the LOPAC®1280 library, were screened at 10 μM single dose. The quality and robustness of the screen were evaluated as described by Zhang et al. (1999) and Iversen et al. (2006) using positive and negative control data. All assay plates met the respective acceptance criteria (Supplementary Table S2).

The primary screen identified 66 hit compounds with $\geq$ twofold induction, all of which, except six previously described CAR ligands, were subjected to a secondary hit confirmation using the same assay and plate format. Table 1 shows the ten confirmed hits, representing potential novel CAR3 ligands. The confirmed hits comprise three retinoids, as well as seven further compounds, which have not yet been associated with CAR. Clopidogrel, which only reached 1.8-fold induction in the hit confirmation, was included due to its pharmacological importance as an essential medicine (WHO 2017). Additionally, Table 1 lists the five previously identified CAR1 agonists and the CAR1 inverse agonist clotrimazole, which were also proven to be CAR3 activators here.

Nine compounds, including three known CAR1 agonists, two retinoids, the top three of the novel compounds and clopidogrel, were selected for an independent powder confirmation. To control for potential cell-type and gene/promoter-specific effects in ligand-dependent CAR3 activation, the hepatic cell line HepG2, which was transiently co-transfected with the CYP2B6 reporter, was used here instead. The novel compounds clemizole, mitotane and sulconazole demonstrated CAR3-dependent induction of CYP2B6 reporter activity, as did permethrin, artemether and the positive control CITCO, while the retinoids bexarotene and alitretinoin showed effects even in the absence of CAR3 (Fig. 1a). Supplementary Fig. S1 shows that the induction of CYP2B6 reporter activity by these retinoids was exclusively dependent on RXRα. Phenoxybenzamine and clopidogrel also showed CAR3-dependent induction, which, however, was only significant in paired t test analyses (results of analysis not shown). In HepG2 cells, clemizole and clopidogrel did not show any cytotoxicity up to 100 μM, while mitotane and sulconazole were cytotoxic at doses larger than 50 μM and 30 μM, respectively (data not shown). In, respectively, guided dose response analyses, all of the four novel compounds proved to activate CAR3 dose-dependently (Fig. 1b).

The CAR3 assay is generally suitable for the identification of CAR agonists

In a previous HTS, ten CAR1 agonists have been specified (Lynch et al. 2015). Five of these were also present in the libraries, which we screened for CAR3 ligands. Of these, phenoxybenzamine and imperatorin were also identified here, while apomorphine, phenelzine and tracazolate did not emerge as hits in our primary screen. When we retested the latter three compounds plus vatalanib, which has also been described as CAR1 agonist (Lynch et al. 2015), at doses of 10 and 30 μM with the CYP2B6/CAR3-RXRα assay in HepG2 cells, tracazolate and vatalanib demonstrated CAR3 activation, while apomorphine and phenelzine did not (Fig. 2a). To confirm the previously reported activation of CAR1 by these compounds, the strong constitutive activity of the receptor, which prevents direct analysis of agonist activity, was inhibited by treatment with the inverse agonist CINPA1 (Cherian et al. 2015). Figure 2b shows that tracazolate and vatalanib released inhibition by CINPA1, while apomorphine and phenelzine did not. Thus, the latter two compounds, which did not activate CAR3, were also not active with CAR1. In conclusion, the CAR3 assay detected all proven CAR1 agonists in the screened libraries.

Novel CAR3 ligands also act as agonists of CAR1

Binding of a ligand into the LBP of a nuclear receptor changes the position of helix 12, thereby generating the

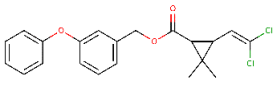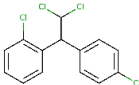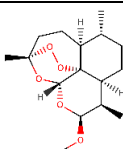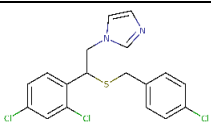**Table 1** Compounds identified as CAR3 activators in HTS
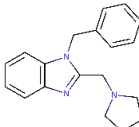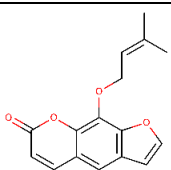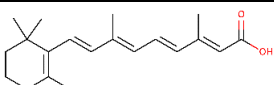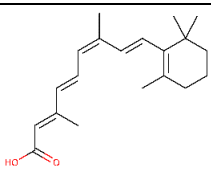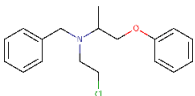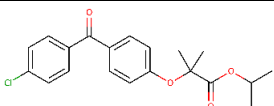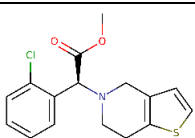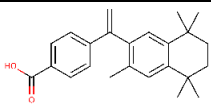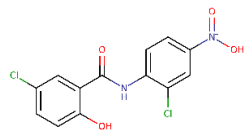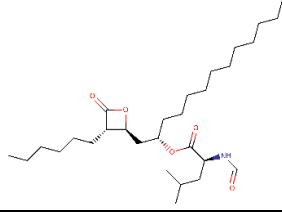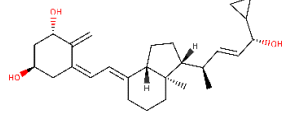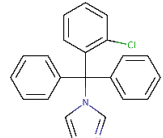
Compound name (CAS no.)	structure	Fold change[a] (PS/HC)	Known NR ligand
Permethrin (52645-53-1)		13.8 / n.d.	CAR, PXR
Mitotane (53-19-0)		9.4 / 4.3	PXR
Artemether (71963-77-4)		8.0 / n.d.	CAR, PXR
Sulconazole (61318-91-0)		4.9 / 2.8	
Clemizole (1163-36-6)		4.7 / 4.1	
Imperatorin (482-44-0)		4.4 /n.d.	CAR, (PXR)
Tretinoin (302-79-4)		4.2 / 3.4	RAR, (RXR)
Alitretinoin (5300-03-8)		3.7 / 4.2	RXR, RAR
Phenoxybenzamine (63-92-3)		2.8 / n.d.	CAR
Fenofibrate (49562-28-9)		2.8 / n.d.	CAR, PPARα
Clopidogrel (120202-66-6)		2.7 / 1.8	
Bexarotene (153559-49-0)		2.7 / 2.9	RXR

Table 1 (continued)

Niclosamide (50-65-7)		2.6 / 2.3	
Orlistat (96829-58-2)		2.5 / 2.6	
Calcipotriene (112965-21-6)		2.2 / 2.4	VDR
Clotrimazole (23593-75-1)		2.0 / n.d.	CAR[b], PXR

In italics, previously known CAR ligands, which emerged as hits in the CAR3 screen

PS primary screen, *HC* hit conformation, *NR* nuclear receptor, *n.d.* not done

[a]As compared to DMSO only

[b]CAR1 inverse agonist and CAR3 agonist

proper coactivator interface. Furthermore, it allosterically affects the position of helix 1, resulting in the stable interaction of this helix with the remainder of the LBD. Two-hybrid nuclear receptor-LBD assembly assays translate this ligand-dependent intramolecular conformational change into the ligand-dependent intermolecular interaction between the helix 1 part and the remainder of the LBD (Pissios et al. 2000). We used the CAR1-LBD assembly assay (Burk et al. 2005b) to analyse whether the novel CAR3 agonists identified here also act as ligands of CAR1. Figure 3a shows that among the novel CAR3 activators, only clopidogrel failed to significantly induce CAR1 LBD assembly. Of the known CAR1 agonists, permethrin and CITCO induced the assembly, while phenoxybenzamine did not. Furthermore, Fig. 3b shows that all newly identified CAR3 agonists resulted in the release of CAR1 inhibition by CINPA1, similarly as did co-treatment with permethrin, phenoxybenzamine and CITCO. Taken together, these data indicate that the newly identified CAR3 activators also act as agonists of CAR1.

Novel agonists induce the translocation of CAR into the nucleus

In primary hepatocytes, ligand binding results in the translocation of CAR1 into the nucleus, while in immortalized cell lines all CAR isoforms show a ligand-independent and predominantly nuclear localization (Yang and Wang 2014).

However, an EGFP-tagged synthetic CAR1 mutant, with insertion of an alanine residue at position 271 (CAR1 + Ala), demonstrated ligand-dependent nuclear translocation in COS1 cells (Chen et al. 2010; Carazo et al. 2018). We first confirmed that the novel agonists act as ligands of the CAR1 + Ala mutant (Supplementary Fig. S2). Subsequently, the compounds were tested in the nuclear translocation assay. All novel agonists resulted in loss of cytoplasmic localization of the EGFP-tagged CAR mutant and enhanced translocation into the nucleus (Supplementary Fig. S3).

Novel agonists differentially induce the interaction of CAR1 and CAR3 with coactivators

CITCO was previously shown to induce the recruitment of coactivators to CAR1 and CAR3 (Arnold et al. 2004). Thus, the respective capacities of the newly identified CAR agonists were analysed by making use of the appropriate mammalian two-hybrid coactivator recruitment assays. Among the novel agonists, only clemizole and mitotane resulted in the recruitment of SRC1 (Fig. 4a) and SRC3 (Fig. 4c) to the LBD of CAR1. Similarly, permethrin and phenoxybenzamine recruited these coactivators to the CAR1-LBD, as did the positive control CITCO. In contrast, only clemizole resulted in the recruitment of SRC1 to the CAR3-LBD (Fig. 4b), while all novel agonists failed to recruit SRC3 to the CAR3-LBD (Fig. 4d). It was previously shown that CITCO strongly
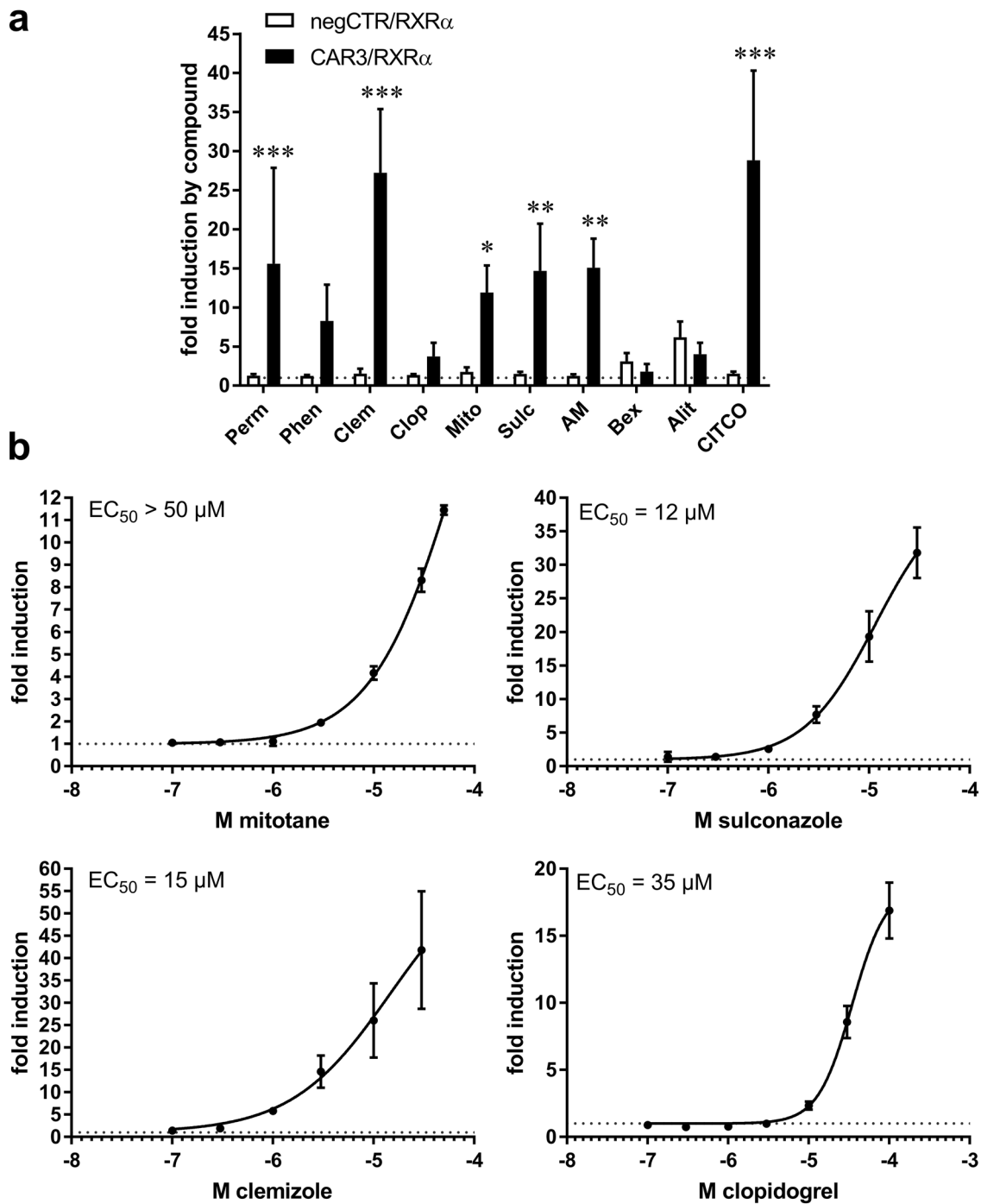
Fig. 1 Confirmation and dose–response analysis of novel CAR3 agonists. **a**, **b** HepG2 cells were co-transfected with expression plasmids encoding RXRα and CAR3 (CAR3/RXRα) or empty vector pcDNA3 (negCTR/RXRα) (**a** only) and treated with the indicated chemicals at 10 μM (**a**) or increasing concentrations (**b**) of the indicated compounds. Permethrin (Perm), phenoxybenzamine (Phen), clemizole (Clem), clopidogrel (Clop), mitotane (Mito), sulconazole (Sulc), artemether (AM), bexarotene (Bex), alitretinoin (Alit). Columns or data points show the mean ± SD ($N \geq 5$, **a**; $N = 3$, **b**) of normalized luciferase activity of co-transfected CYP2B6 reporter relative to, respectively, transfected cells treated with 0.1% DMSO, which was designated 1. Significant differences to, respectively, treated negCTR/RXRα-transfected cells were analysed by ordinary two-way ANOVA with Sidak's multiple comparisons test. *$P < 0.05$; **$P < 0.01$; ***$P < 0.001$
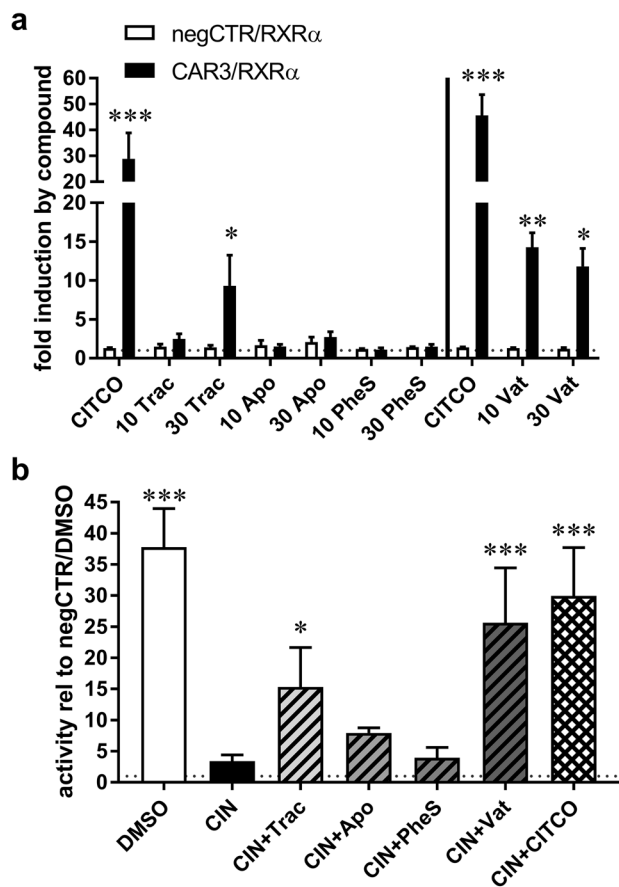
Fig. 2 Retesting of missed CAR1 agonists. a HepG2 cells were co-transfected with expression plasmids encoding RXRα and CAR3 (CAR3/RXRα) or empty vector pcDNA3 (negCTR/RXRα) and treated with the indicated concentrations (in μM) of compounds or with 10 μM CITCO. Tracazolate (Trac), apomorphine (Apo), phenelzine (PheS), vatalanib (Vat). Columns show mean ± SD (N = 3) of normalized luciferase activity of co-transfected CYP2B6 reporter, relative to, respectively, transfected cells treated with 0.1% DMSO, which was designated 1. Significant differences to, respectively, treated negCTR/RXRα-transfected cells were analysed by repeated measures two-way ANOVA with Sidak's multiple comparisons test. b Cells, transfected with CAR1 expression plasmid, were treated with 0.1% DMSO, 2.5 μM CINPA1 (CIN) or combinations of 2.5 μM CINPA1 and 25 μM of the indicated compounds, except for CITCO which was used at 1 μM. Columns show mean ± SD (N ≥ 3) of normalized luciferase activity of co-transfected CYP2B6 reporter, relative to cells, which were transfected with empty vector pcDNA3 (negCTR) and treated with DMSO, which was designated 1. Significant differences to treatment with CINPA1 only were analysed by ordinary one-way ANOVA with Dunnett's multiple comparisons test. *P < 0.05; **P < 0.01; ***P < 0.001

Fig. 3 Novel CAR3 agonists also activate CAR1. a HepG2 cells were co-transfected with expression plasmids encoding GAL4-DBD/hCAR-LBD (105–150) and VP16-AD/hCAR1-LBD (151–348) fusion proteins (CAR1(151–348)) or empty vector pVP16-AD (AD) and treated with 10 μM of the indicated compounds (abbreviations as in Fig. 1). Columns show mean ± SD (N = 5) of normalized luciferase activity of co-transfected reporter pGL3-G5, relative to, respectively, transfected cells treated with 0.1% DMSO, which was designated 1. Significant differences to, respectively, treated cells, which were transfected with pVP16-AD only, were analysed by repeated measures two-way ANOVA with Sidak's multiple comparisons test. b HepG2 cells, transfected with CAR1 expression plasmid, were treated with 0.1% DMSO, 2.5 μM CINPA1 (CIN) or combinations of 2.5 μM CINPA1 and 25 μM of the indicated compounds, except for CITCO which was used at 1 μM. Columns show mean ± SD (N = 5) of normalized luciferase activity of co-transfected CYP2B6 reporter, relative to cells, which were transfected with empty vector pcDNA3 (negCTR) and treated with DMSO, which was designated 1. Significant differences to treatment with CINPA1 only were analysed by repeated measures one-way ANOVA with Dunnett's multiple comparisons test. *P < 0.05; **P < 0.01; ***P < 0.001

induced the recruitment of coactivator DRIP205 (MED1) to CAR3, while only modestly inducing the recruitment to CAR1 (Arnold et al. 2004). DRIP205 represents the nuclear receptor interacting component of the mediator complex. Among the novel agonists, only mitotane failed to induce the recruitment of DRIP205 to CAR3, similarly as did phenoxybenzamine (Fig. 4e). On the other hand, only CITCO recruited DRIP205
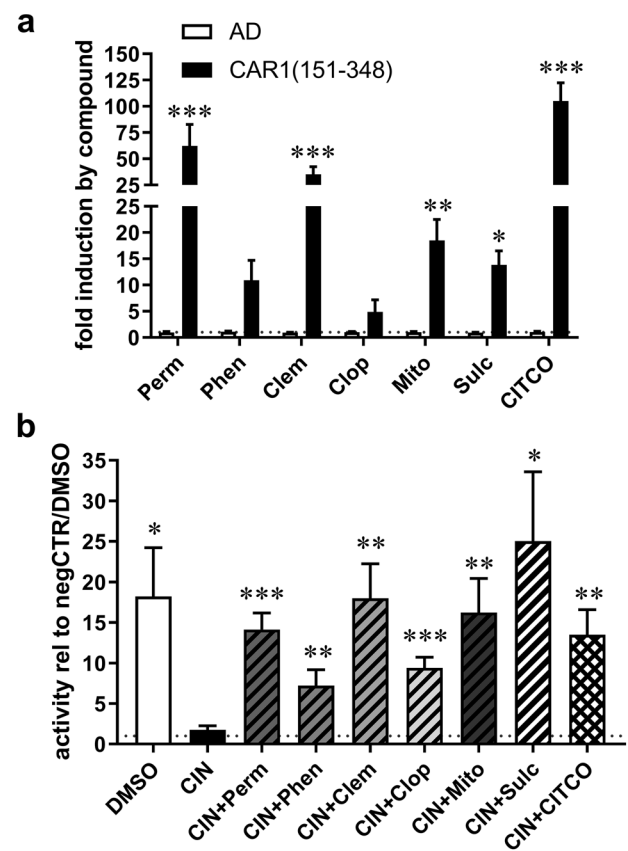
to CAR1. In conclusion, these data demonstrate both isoform- and ligand-specific interaction of coactivators with CAR.

Novel agonist clemizole interacts in vitro with the CAR1 LBD

In vitro analysis of ligand binding of the novel CAR agonists was done using respective CARLA. The assay relies on
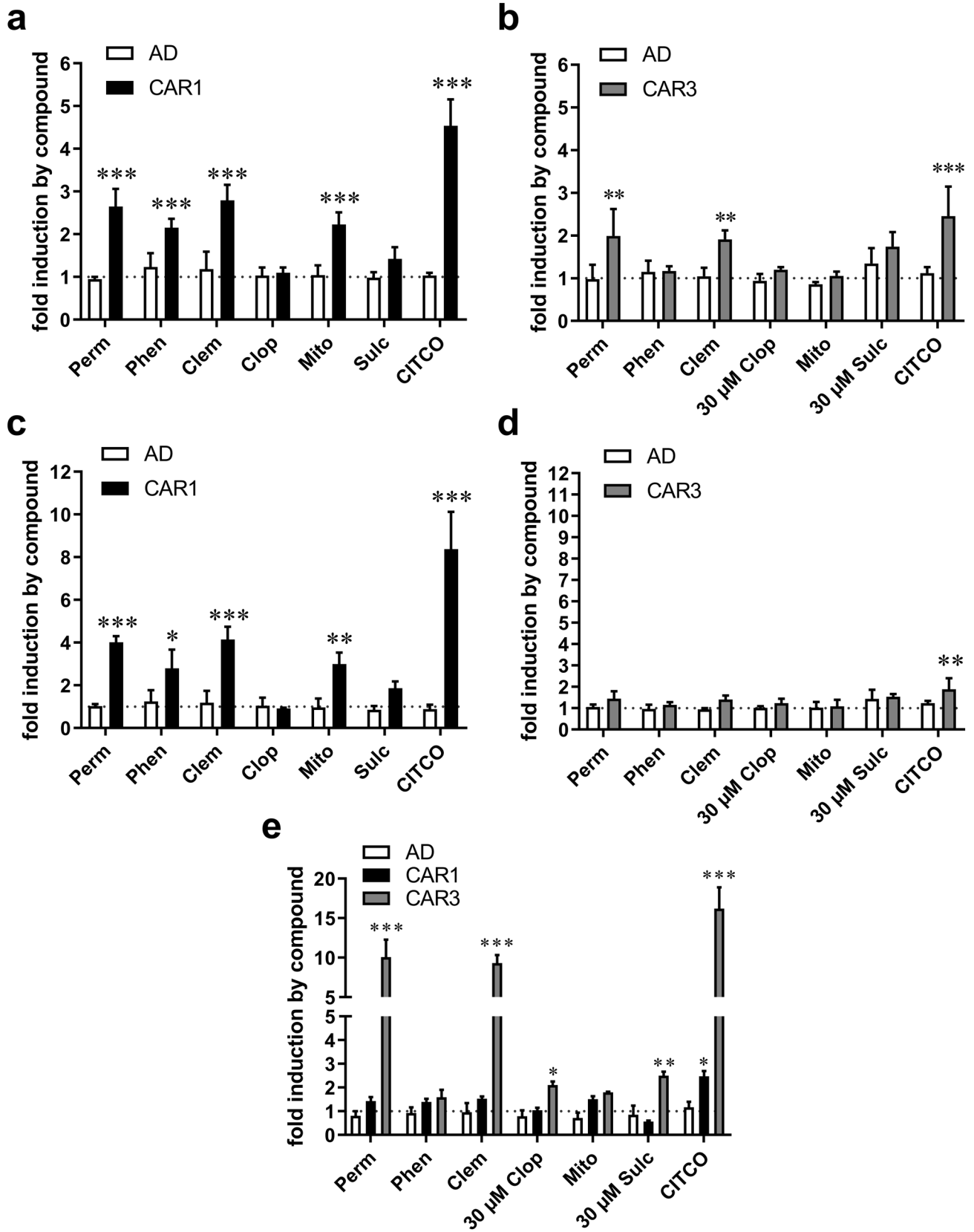
◄**Fig. 4** Novel agonists differentially induce the interaction of CAR isoforms with coactivators. HepG2 cells were co-transfected with expression plasmids encoding GAL4-DBD/SRC1-RID (583–783) (**a**, **b**), GAL4-DBD/SRC3-RID (582–782) (**c**, **d**) or GAL4-DBD/DRIP205-RID (527–774) (**e**) and VP16-AD/hCAR1-LBD (105–348) (CAR1), VP16-AD/hCAR3-LBD (105–353) (CAR3) fusion proteins or empty vector pVP16-AD (AD). Transfected cells were treated with 10 μM of the indicated compounds (abbreviations as in Fig. 1), if not indicated otherwise, or with 1 μM CITCO. Columns show mean $\pm$ SD ($N = 3$, **a–d**; $N \geq 3$, **e**) of normalized luciferase activity of co-transfected reporter pGL3-G5, relative to, respectively, transfected cells treated with 0.1% DMSO, which was designated 1. Significant differences to, respectively, treated cells, which were transfected with pVP16-AD only, were analysed by repeated measures (**a–d**) or ordinary (**e**) two-way ANOVA with Sidak's or Dunnett's multiple comparisons test, respectively. *$P < 0.05$; **$P < 0.01$; ***$P < 0.001$

the ligand-dependent interaction of radiolabeled full-length CAR1 with the bacterially expressed RID of coactivator SRC1 (Burk et al. 2012). Figure 5 shows that among the novel CAR agonists, only clemizole induced the interaction of SRC1 and CAR1 in vitro. Effects of the other three were only significant, if individually compared to DMSO by paired t test (results of analysis not shown). While permethrin and CITCO also strongly induced the interaction, phenoxybenzamine rather seemed to reduce it.

CAR activation by clopidogrel is not mediated by the major inactive metabolite

Clopidogrel is the only compound of outstanding pharmacological importance among the novel CAR agonists. The pro-drug is extensively metabolized, mainly by hepatic carboxylesterase (CES) 1, which generates the major and pharmacologically inactive carboxylic acid metabolite (Tang et al. 2006). As CES1 expression and metabolic activity have been monitored in HepG2 cells (Liu et al. 2014), the carboxylic acid metabolite may actually mediate CAR activation. However, treatment with up to 100 or 50 μM clopidogrel carboxylic acid neither activated CAR3, nor revoked inhibition of CAR1 by CINPA1, respectively (Supplementary Fig. S4). As HepG2 cells mostly lack xenobiotic-metabolizing cytochrome P450 enzymes (Wilkening et al. 2003), which generate the minor active metabolite (Hagihara et al. 2009), it can be concluded that the activation of CAR results from parental clopidogrel.

Novel CAR agonists also activate PXR and differentially induce ADME gene expression in primary human hepatocytes

Several compounds, e.g. artemisinin and its derivatives (Burk et al. 2005b), activate both CAR and PXR. Therefore, an analysis was carried out to determine whether the newly identified CAR agonists also activate PXR. With the exception of clopidogrel, all novel CAR agonists demonstrated activation of PXR in the CYP3A4 reporter assay, as did permethrin and phenoxybenzamine (Fig. 6). The carboxylic acid metabolite of clopidogrel failed to activate PXR (Supplementary Fig. S5).

The induction of endogenous ADME gene expression was analysed in primary human hepatocytes. Figure 7 shows that the four novel CAR agonists induced CYP2B6 gene expression in hepatocytes of all three donors. CYP3A4 was induced by all four novel CAR agonists in hepatocytes of only two donors. ABCB1 was induced by mitotane in hepatocytes of two donors and by sulconazole in hepatocytes of one donor. The preferential induction of the prototypical CAR target gene CYP2B6 further confirms activation of CAR by these compounds. As it was shown that CAR also participates in the down-regulation of gluconeogenic and lipogenic genes (Yan et al. 2015), we further analysed the modulation of the gluconeogenic genes PCK1, G6PC and of the lipogenic genes FASN, SCD and THRSP by the novel agonists. In contrast to ADME gene regulation, effects on these genes were first of all only modest and second not in the same direction for all CAR ligands (Supplementary Fig. S6), which strongly argues against a dominant role of CAR in mediating the effects of the novel agonists on these genes. Only mitotane resulted in the expected down-regulation of all genes.

Molecular modeling of CAR3

Based on a homology model of CAR3, it has been suggested that the insertion of the five amino acids APYLT does not change ligand-binding specificity as compared to CAR1 (Auerbach et al. 2003 Omiecinski et a. 2011). However, a detailed analysis of the impact of the five amino acid insert on the LBD structure, the LBP volume, as well as the heterodimerisation surface is still missing. Therefore, we generated a homology model of CAR3 in complex with RXRα using the CAR1/RXRα X-ray crystal structure (PDB 1XVP) as template. A comparison of the CAR1 and CAR3 structures shows that the five amino acids' insertion results in disruption of several salt bridges, both within the CAR LBD and shared with RXRα (Fig. 8a). In the CAR1 X-ray crystal structure, E200 forms a bidentate salt bridge with R272 (R277 in CAR3) as well as a water-mediated hydrogen bond with R320 (R325 in CAR3) that in turn shares a charged hydrogen bond with S427 on RXRα (Fig. 8a). Also D271 (D276 in CAR3) of CAR1 forms a bidentate salt bridge with R320 on the same protein (R325 in CAR3) and a salt bridge with R348 on RXRα. In the CAR3 model, the salt bridge between E200 and R277 was unable to form due to relocation of R277 upon introduction of the APYLT insertion. For the same reason, a salt bridge was not established between D276 and R325.
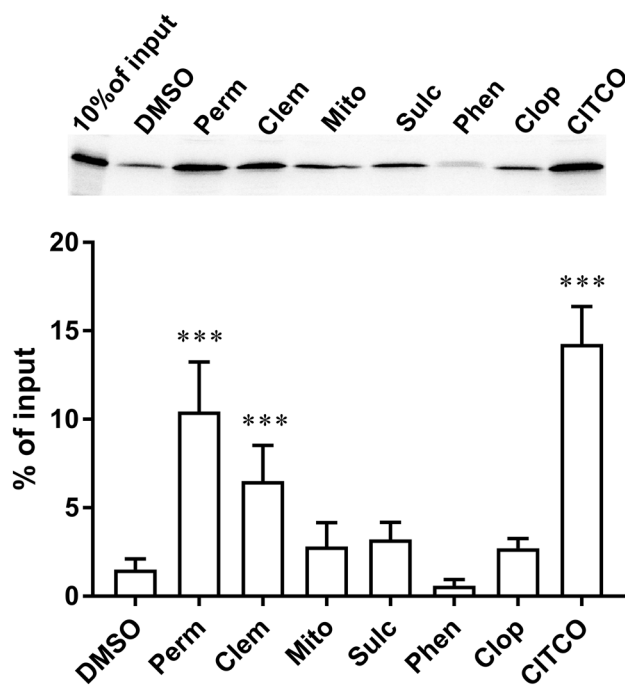
Fig. 5 In vitro interaction of novel compounds with CAR1. Ligand-dependent induction of the interaction of bacterially expressed GST/SRC1-RID with ^{35}S-Met labelled full-length human CAR1 protein, was analysed by CARLA. Quantification of the pulled down CAR1 protein was done by radioluminography of protein gels. The assay was carried out in the presence of solvent DMSO only (1%), 10 μM CITCO, 100 μM permethrin (Perm) or clemizole (Clem) or 300 μM mitotane (Mito), sulconazole (Sulc), phenoxybenzamine (Phen) or clopidogrel (Clop). Upper panel, scanning image of a representative experiment; lower panel, quantitative analysis with columns showing mean ± SD of three to five independent experiments with respect to input. Significant differences to incubation with DMSO only were analysed by ordinary one-way ANOVA with Dunnett's multiple comparisons test. ***$P < 0.001$

In order to compare the structural dynamics of the CAR1 X-ray crystal structure and the CAR3 homology model, which are structurally identical except the α8-α9 loop, molecular dynamics (MD) simulations of 500 ns length were carried out for both LBD structures. A comparison of the two structures resulting from the 500-ns simulation revealed only minor differences in the secondary structural elements (Fig. 8b). The overall root–mean–square deviation (RMSD) of Cα atoms was 2.1 Å and reduced to 1.5 Å when increasing the weights of residues located in α-helices and the β-strand for structural superpositioning. While the α8–α9 loop in CAR1 remained almost unchanged, its conformation in CAR3 significantly differed from the starting geometry. Structural superpositioning of the CAR3 model on the CAR1/RXRα X-ray crystal structure (PDB ID 1XVP) showed interference between the CAR3 α8-α9 loop and amino acids located on α6 and α10/11 of RXRα.
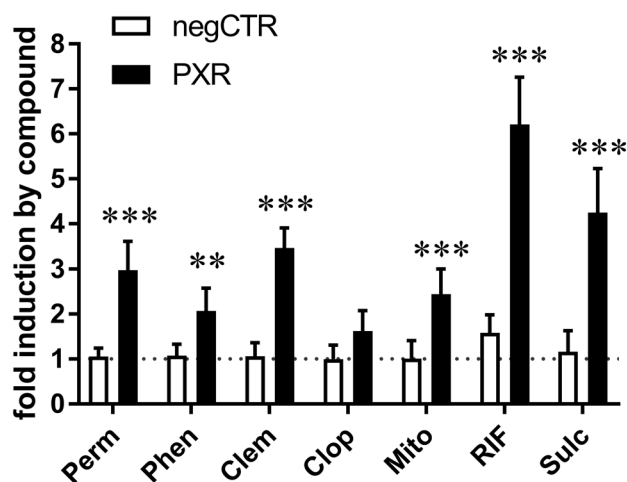

Fig. 6 Novel CAR agonists crosstalk with PXR. HepG2 cells, transfected with empty vector pcDNA3 (negCTR) or PXR expression plasmid, were treated with 10 μM of the indicated chemicals (abbreviations as in Fig. 1). Columns show mean ± SD ($N = 5$) of normalized luciferase activity of co-transfected CYP3A4 reporter, relative to, respectively, transfected cells treated with 0.1% DMSO, which was designated 1. Significant differences to, respectively, treated negCTR cells were analysed by repeated measures two-way ANOVA with Sidak's multiple comparisons test. **$P < 0.01$; ***$P < 0.001$

RMSD calculations for Cα atoms during the course of the MD simulations revealed a slightly higher average value for CAR3 (1.8 Å) compared to CAR1 (1.5 Å) (Fig. 9a). For a more detailed analysis of the LBD flexibility, the root–mean–square fluctuations (RMSF) of Cα atoms were calculated for each residue. The plots revealed a significantly larger flexibility of residues 270–285 in CAR3, belonging to the α8–α9 loop which contains the APYLT insertion (Fig. 9b). All other regions of both receptors did not show any pronounced differences. In order to investigate whether the extended α8–α9 loop results in changes of the LBP size, the volume was calculated for all MD frames (Fig. 9c). Starting at ~800 Å^3, the LBP volumes of both receptors shrank at the beginning of the simulations and then remained very stable. For CAR1, the mean volume was 616 Å^3, while for CAR3 the LBP revealed as slightly larger with a mean volume of 656 Å^3. Also the solvent-accessible surface area (SASA) of the LBPs as well as the polar and non-polar SASA contributions did not vary significantly between both receptors (Supplementary Table S3). Moreover, the stability of the salt bridges involving residues of the α8–α9 loop was investigated. While in CAR1 the salt bridges E200-R272 and D271-R320 remained stable throughout the course of the simulation, the corresponding amino acids in CAR3 did not show any such interaction (Fig. 9d).

Finally, we investigated any impact of the extended α8-α9 loop in CAR3 on the C-terminal α12 helix. At first, any direct interactions between the receptors and residues

Fig. 7 Novel CAR agonists differentially affect the expression of ▶ ADME genes in primary human hepatocytes. Cultures of primary human hepatocytes, derived from donors GH56, GH57 and GH58, were treated for 24 h with 0.1% DMSO, 1 μM CITCO, 30 μM clemizole, mitotane or sulconazole, or 100 μM clopidogrel (abbreviations as in Fig. 1). The expression of ABCB1, CYP2B6 and CYP3A4 was analysed in respective total RNA samples by RT-qPCR and normalized with respect to the expression of 18S rRNA. Columns show mean fold induction ± SD ($n = 3$, technical replicates) by chemical treatment, as compared to the mean of treatment with DMSO. Significant differences of treatments to respective DMSO treatments were analysed by ordinary two-way ANOVA with Dunnett's multiple comparisons test. $*P < 0.05$; $**P < 0.01$; $***P < 0.001$

341–348 (CAR1, CAR3: 346–353) were analysed. While for CAR1 no persistent interaction emerged, CAR3 revealed few persistent contacts (Supplementary Fig. S7a). However, these interactions neither influenced the position of the helix in terms of RMSD, nor substantially influenced the number of α-helical residues (Supplementary Fig. S7b, c).

Molecular docking of novel agonists into the LBP of CAR

In addition, the potential binding modes of the newly identified CAR3 agonists were investigated using molecular docking. Due to the very limited differences in the LBP volumes of CAR1 and CAR3, as observed in the MD simulations, CAR1 X-ray crystal structures (PDB ID 1XV9, 1XVP) were used for the docking approach. All six compounds were docked into the four LBPs using GOLD with the ChemPLP scoring function. For permethrin, phenoxybenzamie, and sulconazole, all possible enantiomers, and for clemizole and sulconazole, two protomers were docked. The results revealed all compounds to bind with similar ligand efficacy (= docking score/number of heavy atoms) to CAR1 compared to the known agonist CITCO (Supplementary Table S4). Remarkably, all top-ranked docking poses emerged for both CAR protein structures in PDB ID 1XVP.

Discussion

Screening two libraries, with together 2054 compounds, for activators of the ligand-dependent isoform CAR3 resulted in the identification of novel agonists and further proved that the CAR3 HTS assay was generally suitable for screening for CAR agonists. Four of the novel agonists were characterized further and proved also to activate CAR1. Induction of nuclear translocation and coactivator interaction and molecular docking, as well as preferential induction of the prototypical CAR target gene CYP2B6, further confirmed that these compounds bind to and activate CAR.

The CAR3 assay seems to be generally suitable for the identification of CAR agonists, as the previously identified
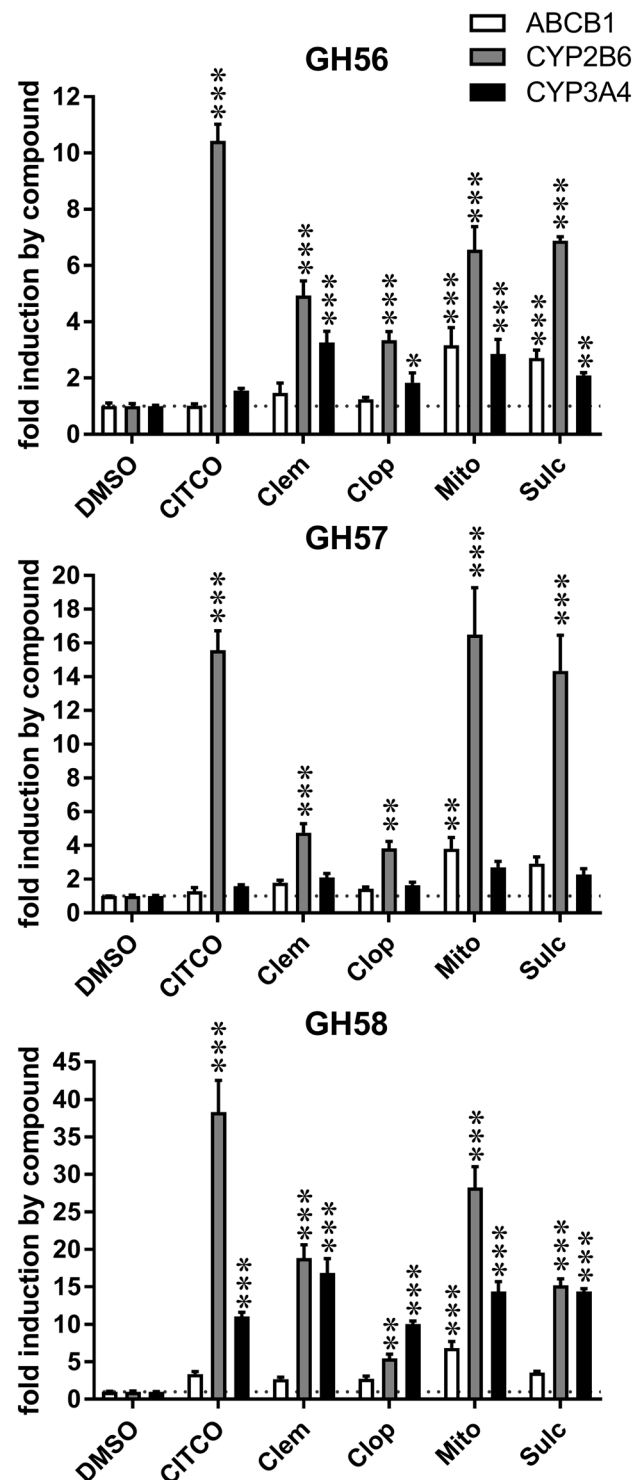
CAR1 agonists permethrin, fenofibrate (Küblbeck et al. 2011), imperatorin, phenoxybenzamine (Lynch et al. 2015) and artemether (Burk et al. 2012) also proved to activate CAR3 in HTS. The failure to recognize single CAR1 agonists can be explained either by agonists having only small effects at the screening dose of 10 μM, as in the case of tracazolate, or by the presence of false positives in the listing of
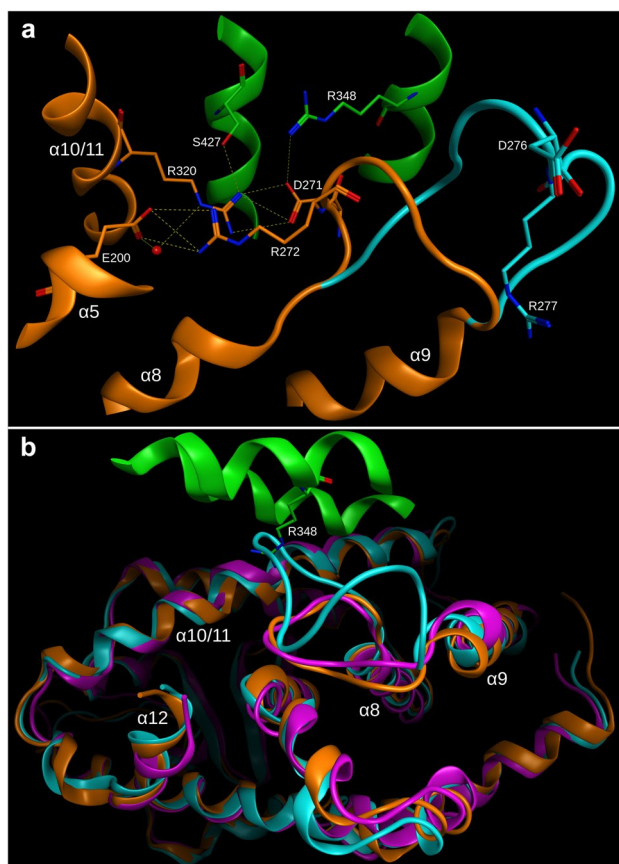
Fig. 8 Structural comparison of CAR1 X-ray crystal structure (PDB ID 1XVP, orange) and the CAR3 homology model (cyan). RXRα is shown in green. **a** Selected hydrogen bonds and salt bridges within the CAR LBD or shared with RXRα (carbon atoms in orange) are shown as yellow dotted lines. Parts of the receptor structures were removed for clarity. **b** Superpositioning of the CAR1 (pink) and CAR3 (cyan) structure after the 500-ns simulation onto CAR1/RXRα X-ray crystal structure

CAR1 agonists by Lynch et al. (2015). According to the data presented here, apomorphine and phenelzine, which have been described as CAR1 agonists by Lynch et al. (2015), may be false positives (see Fig. 2b). Interestingly, these two compounds also failed to translocate CAR into the nucleus of primary hepatocytes (Lynch et al. 2015), which is characteristic of CAR activators. Alternatively, the divergent results may stem from the use of different inverse agonists in the CAR1 assay. While PK11195 has been used by Lynch et al. (2015), we employed CINPA1 as an inverse agonist due to its proven higher potency than PK11195 (Cherian et al. 2015). The two inverse agonists differ from each other with regard to cofactor interactions: corepressor SMRT is only recruited to CAR by CINPA1 (Li et al. 2008; Cherian et al. 2015). In conclusion, it can be expected that the CAR3 assay will detect the large majority of, if not all, CAR1 agonists, as we failed to detect exclusive activation of CAR1 by any of the tested compounds.

Besides CAR agonists, the CAR3 assay may also detect CAR1 inverse agonists as agonists, which is demonstrated here by the identification of clotrimazole as a hit compound. In this regard, the CAR3 assay acted similar to the previously described mammalian one-hybrid screening assay, based on a ligand-dependent CAR-LBD mutant, which also identified the inverse agonists clotrimazole and PK11195 as agonists (Kanno and Inouye 2010). Recently, ten novel inverse agonists have been described (Lynch et al. 2015), seven of which were also present in the compound libraries used here. As none of these turned out as a hit in the CAR3 assay, it can be concluded that this assay is not generally suitable for the detection of CAR1 inverse agonists, even if single ones, such as clotrimazole (Auerbach et al. 2005; this study) and NF49 (Anderson et al. 2011), activate CAR3.

The major limitation of the CAR3 assay is the reliance on overexpression of RXRα. Given that commonly used cytochrome P450-based reporters demonstrate induction by activated RXRα only (see Supplementary Fig. S1), this results in hits, which actually represent RXRα ligands. Thus, it is obligatory to incorporate appropriate negative controls into the follow-up investigations to exclude these. Hereby, alitretinoin and bexarotene were rejected as CAR3 agonists. However, appropriate negative controls in follow-up investigations are necessary anyway to exclude false positive hits due to compound-only effects on assay systems. Altogether, the CAR3 assay has the clear advantage that it makes use of an abundant natural ligand-dependent CAR isoform and does neither require fusion to a foreign DBD nor the concomitant use of an inverse agonist, which both may influence the outcome.

All four novel CAR3 agonists also activated CAR1, meaning that we did not detect any CAR3-selective compound in our screen. Pheniramine, which was previously reported to selectively activate CAR3 (Dring et al., 2010), was present in one of the screened libraries, but did not emerge as a hit. Furthermore, and in contradiction to Dring et al. (2010), we failed to verify activation of CAR3 by pheniramine (data not shown). The conflicting result may have arisen from the use of a mammalian one-hybrid assay, which is based on a fusion of the GAL4-DBD with CAR, and/or a different cell line (Huh7) by Dring et al. (2010). Alternatively, pheniramine may simply represent a false positive hit in their study, as compound-only effects had not been addressed. The failure to identify CAR3-specific ligands, which is further explained by the molecular modelling data (see below), implies that a specific pharmacological modulation of CAR3 activity may not be possible at all. However, the physiological relevance of the isoform is suggested by its high hepatic abundance (Ross et al. 2010) and a specific role in the control of hepatic gene expression also suggested by its peculiar interaction mechanism with RXRα (Auerbach et al. 2005). Further investigations are clearly required but
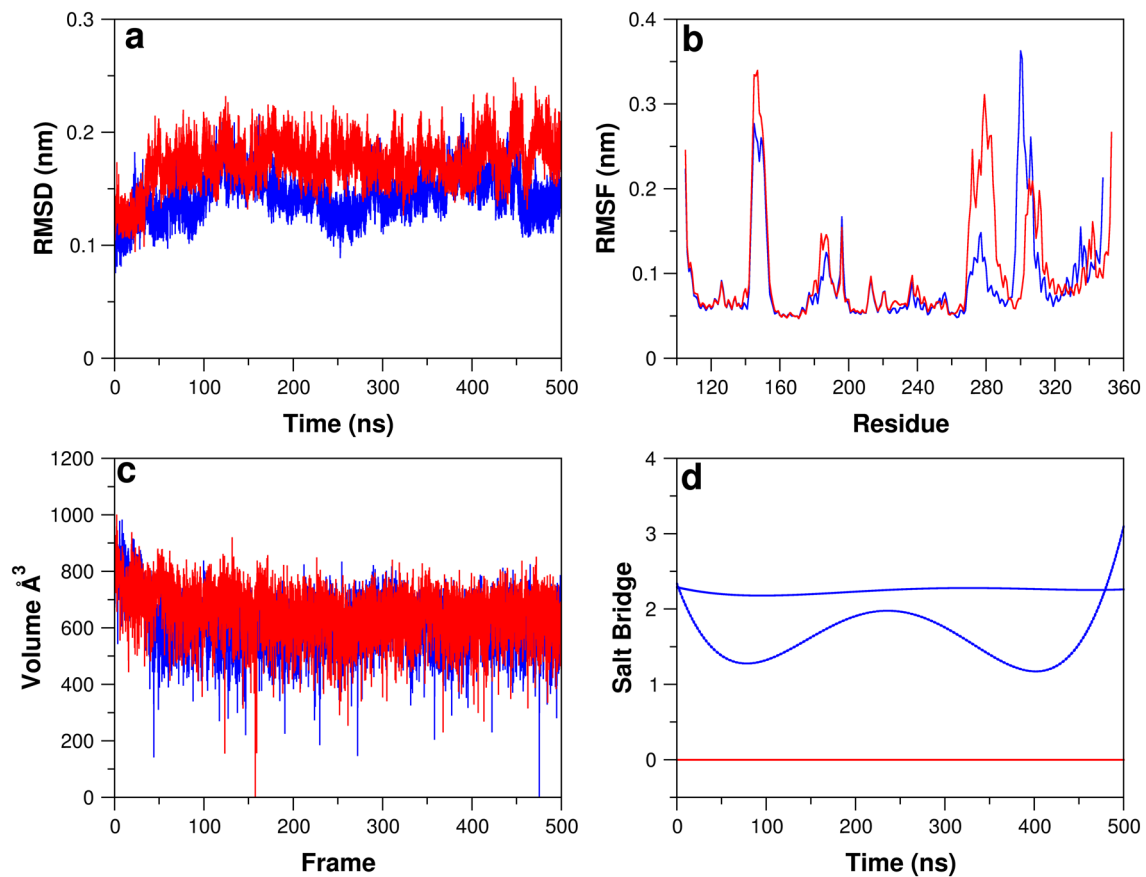
Fig. 9 CAR1 (blue) and CAR3 (red) molecular dynamics simulations. **a** RMSD plot for Cα atoms. **b** Root–mean–square fluctuation for Cα atoms **c** Mean LBP volume for each frame of the simulation. **d** Salt bridge occurrence between E200 and R272 (blue line) as well as D271 and R320 (blue dotted line) and the corresponding interactions in CAR3 (E200 and R277, D276 and R325, red lines)

have to rely on techniques such as, e.g. siRNA-mediated knock-down.

Among the four novel CAR agonists, which have been investigated here in more detail, mitotane, a drug used to treat adrenocortical carcinoma, and the anti-thrombogenic medication clopidogrel are of special interest. Mitotane is a known inducer of CYP3A4 and was shown to decrease plasma levels of co-administered sunitinib (van Erp et al. 2011) and to autoinduce its own metabolism, which may result in therapeutic failure (Arshad et al. 2018). Theile et al. (2015) demonstrated that mitotane activates PXR. In that and in the autoinduction of metabolism mitotane joins the anti-malarial drug artemisinin, which also has been shown to induce its own metabolism by induction of CYP2B6 (Simonsson et al. 2003) and to activate CAR and PXR (Burk et al. 2005b). Due to the dual activation of CAR and PXR, the specific contribution of CAR to the clinical effects of autoinduction is unknown. Clopidogrel, which is itemized on WHO's essential medicine list (WHO 2017) activated CAR and induced CYP3A4 and CYP2B6 in primary hepatocytes. The compound is metabolized by hepatic carboxylesterase

CES1 to the inactive carboxylic acid metabolite (Tang et al. 2006), which represents 90% of total metabolites (Hagihara et al. 2009) and did not activate CAR and PXR in this study. The parental pro-drug is rapidly cleared and only detectable at low nanomolar concentrations in plasma (Karaźniewicz-Łada et al. 2014). As CAR activation in HepG2 and ADME gene induction in primary human hepatocytes required high micromolar concentrations of clopidogrel, it is, therefore, most likely not of clinical relevance. However, in situations of CES1 deficiency, either by chemical inhibition or genetic variation, where increased levels of parental clopidogrel have to be expected, CAR activation may be conceivable and further result in the induction of cytochrome P450 expression. Consequently, the CYP-dependent metabolism of clopidogrel and/or of co-administered drugs would be enhanced, which may finally impact on therapeutic drug efficiency. In support of this conception, it has been shown in vitro that chemical inhibition of CES1 in liver microsomes resulted in fivefold increase of clopidogrel area under the concentration–time curve (AUC) (Zhu et al. 2013). Similarly, heterozygous carriers of the CES1 single nucleotide

polymorphism c.428G > A, which results in the catalytically deficient protein variant G143E, demonstrated doubled clopidogrel maximal plasma concentration and AUC (Tarkiainen et al. 2015).

To better understand the structural consequences of the APYLT insertion in CAR3, a comprehensive in silico analysis was carried out. The previous molecular modelling studies neither considered the CAR3-RXRα interactions nor made use of molecular dynamics simulations for studying the impact of the extended α8-α9 loop on the LBP. Our results confirmed the previous observation that the APYLT insertion does not significantly influence the LBP (Omiecinski et al. 2011). Instead, the simulations suggest that the loop extension in CAR3 impairs heterodimerization with RXRα. Experimental evidence for impaired interaction with RXRα has already been presented (Arnold et al. 2004). Moreover, the disrupted salt bridges and hydrogen bonds involving residues in the α8–α9 region and their interaction partners in CAR and RXRα may influence dimerization. At first sight, the impaired heterodimerization potential of CAR3 poses a problem for the understanding of the potentiating effect of RXRα on CAR3 transactivation activity. However, it has already been shown that this effect does not require classical heterodimerization of CAR3 with RXRα, but may result from enhanced interaction with coactivators (Auerbach et al. 2005). The precise molecular mechanism has not yet been elucidated. Our results do not support the previously suggested disruption of the α12 helix position by the extended α8–α9 loop as an explanation for the loss of constitutive activity of CAR3 (Omiecinski et al. 2011). Further simulations involving the CAR/RXRα heterodimer are needed for better understanding the differences in the interaction of CAR1 and CAR3 with RXRα.

Molecular docking revealed all newly identified CAR3 agonists to favourably bind to the CAR1 X-ray crystal structures. Ligand efficiency scores similar to the known agonist CITCO indicate potential usage of the chosen method in virtual screening campaigns for novel CAR1 and/or CAR3 agonists.

Altogether, our study proved the usability of the CAR3 HTS assay for the identification of novel CAR agonists. It indicated that CAR3 performs comparable to CAR1 in agonist screening, but did not provide any evidence, neither in vitro nor in silico, for the existence of CAR3-selective ligands. The CAR3 HTS assay is thus suitable for generally screening for CAR agonists and represents a convenient alternative to previously used screening assays.

Compliance with ethical standards

References

Anderson LE, Dring AM, Hamel LD, Stoner MA (2011) Modulation of constitutive androstane receptor (CAR) and pregnane X receptor (PXR) by 6-arylpyrrolo[2,1-d][1,5]benzothiazepine derivatives, ligands of peripheral benzodiazepine receptor (PBR). Toxicol Lett 202:148–154. https://doi.org/10.1016/j.toxlet.2011.02.004

Arnold KA, Eichelbaum M, Burk O (2004) Alternative splicing affects the function and tissue-specific expression of the human constitutive androstane receptor. Nucl Recept 2:1. https://doi.org/10.1186/1478-1336-2-1

Arshad U, Taubert M, Kurlbaum M et al (2018) Enzyme autoinduction by mitotane supported by pharmacokinetic modeling in a large cohort of adrenocortical carcinoma patients. Eur J Endocrinol 179:287–297. https://doi.org/10.1530/EJE-18-0342

Auerbach SS, Ramsden R, Stoner MA et al (2003) Alternatively spliced isoforms of the human constitutive androstane receptor. Nucleic Acids Res 31:3194–3207. https://doi.org/10.1093/nar/gkg419

Auerbach SS, Stoner MA, Su S, Omiecinski CJ (2005) Retinoid X receptor-alpha-dependent transactivation by a naturally occurring structural variant of human constitutive androstane receptor (NR1I3). Mol Pharmacol 68:1239–1253. https://doi.org/10.1124/mol.105.013417

Bitter A, Rümmele P, Klein K et al (2015) Pregnane X receptor activation and silencing promote steatosis of human hepatic cells by distinct lipogenic mechanisms. Arch Toxicol 89:2089–2103. https://doi.org/10.1007/s00204-014-1348-x

Burk O, Arnold KA, Geick A et al (2005a) A role for constitutive androstane receptor in the regulation of human intestinal MDR1 expression. Biol Chem 386:503–513. https://doi.org/10.1515/BC.2005.060

Burk O, Arnold KA, Nussler AK et al (2005b) Antimalarial artemisinin drugs induce cytochrome P450 and MDR1 expression by activation of xenosensors pregnane X receptor and constitutive androstane receptor. Mol Pharmacol 67:1954–1965. https://doi.org/10.1124/mol.104.009019

Burk O, Piedade R, Ghebreghiorghis L et al (2012) Differential effects of clinically used derivatives and metabolites of artemisinin in the activation of constitutive androstane receptor isoforms. Br J Pharmacol 167:666–681. https://doi.org/10.1111/j.1476-5381.2012.02033.x

Burk O, Kuzikov M, Kronenberger T et al (2018) Identification of approved drugs as potent inhibitors of pregnane X receptor activation with differential receptor interaction profiles. Arch Toxicol 92:1435–1451. https://doi.org/10.1007/s00204-018-2165-4

Carazo A, Dusek J, Holas O et al (2018) Teriflunomide is an indirect human constitutive androstane receptor (CAR) activator interacting with epidermal growth factor (EGF) signaling. Front Pharmacol 9:993. https://doi.org/10.3389/fphar.2018.00993

Chen T, Tompkins LM, Li L et al (2010) A single amino acid controls the functional switch of human constitutive androstane receptor (CAR) 1 to the xenobiotic-sensitive splicing variant CAR3. J Pharmacol Exp Ther 332:106–115. https://doi.org/10.1124/jpet.109.159210

Cherian MT, Lin W, Wu J, Chen T (2015) CINPA1 is an inhibitor of constitutive androstane receptor that does not activate pregnane X receptor. Mol Pharmacol 87:878–889. https://doi.org/10.1124/mol.115.097782

DeKeyser JG, Laurenzana EM, Peterson EC et al (2011) Selective phthalate activation of naturally occurring human constitutive androstane receptor splice variants and the pregnane X receptor. Toxicol Sci 120:381–391. https://doi.org/10.1093/toxsci/kfq394

Dring AM, Anderson LE, Qamar S, Stoner MA (2010) Rational quantitative structure-activity relationship (RQSAR) screen for PXR and CAR isoform-specific nuclear receptor ligands. Chem Biol Interact 188:512–525. https://doi.org/10.1016/j.cbi.2010.09.018

Geick A, Eichelbaum M, Burk O (2001) Nuclear receptor response elements mediate induction of intestinal MDR1 by rifampin. J Biol Chem 276:14581–14587. https://doi.org/10.1074/jbc.M010173200

Hagihara K, Kazui M, Kurihara A et al (2009) A possible mechanism for the differences in efficiency and variability of active metabolite formation from thienopyridine antiplatelet agents, prasugrel and clopidogrel. Drug Metab Dispos 37:2145–2152. https://doi.org/10.1124/dmd.109.028498

Hoffart E, Ghebreghiorghis L, Nussler AK et al (2012) Effects of atorvastatin metabolites on induction of drug-metabolizing enzymes and membrane transporters through human pregnane X receptor. Br J Pharmacol 165:1595–1608. https://doi.org/10.1111/j.1476-5381.2011.01665.x

Iversen PW, Eastwood BJ, Sittampalam GS, Cox KL (2006) A comparison of assay performance measures in screening assays: signal window, Z' factor, and assay variability ratio. J Biomol Screen 11:247–252. https://doi.org/10.1177/1087057105285610

Jeske J, Windshügel B, Thasler WE et al (2017) Human pregnane X receptor is activated by dibenzazepine carbamate-based inhibitors of constitutive androstane receptor. Arch Toxicol 91:2375–2390. https://doi.org/10.1007/s00204-017-1948-3

Jiang M, Xie W (2013) Role of the constitutive androstane receptor in obesity and type 2 diabetes: a case study of the endobiotic function of a xenobiotic receptor. Drug Metab Rev 45:156–163. https://doi.org/10.3109/03602532.2012.743561

Jinno H, Tanaka-Kagawa T, Hanioka N et al (2004) Identification of novel alternative splice variants of human constitutive androstane receptor and characterization of their expression in the liver. Mol Pharmacol 65:496–502. https://doi.org/10.1124/mol.65.3.496

Kandel BA, Thomas M, Winter S et al (2016) Genomewide comparison of the inducible transcriptomes of nuclear receptors CAR, PXR and PPARα in primary human hepatocytes. Biochim Biophys Acta 1859:1218–1227. https://doi.org/10.1016/j.bbagrm.2016.03.007

Kanno Y, Inouye Y (2010) A consecutive three alanine residue insertion mutant of human CAR: a novel CAR ligand screening system in HepG2 cells. J Toxicol Sci 35:515–525

Karaźniewicz-Łada M, Danielak D, Burchardt P et al (2014) Clinical pharmacokinetics of clopidogrel and its metabolites in patients with cardiovascular diseases. Clin Pharmacokinet 53:155–164. https://doi.org/10.1007/s40262-013-0105-2

Küblbeck J, Laitinen T, Jyrkkärinne J et al (2011) Use of comprehensive screening methods to detect selective human CAR activators. Biochem Pharmacol 82:1994–2007. https://doi.org/10.1016/j.bcp.2011.08.027

Lamba J, Lamba V, Schuetz E (2005) Genetic variants of PXR (NR1I2) and CAR (NR1I3) and their implications in drug metabolism and pharmacogenetics. Curr Drug Metab 6:369–383. https://doi.org/10.2174/1389200054633880

Laskowski RA, MacArthur MW, Moss DS, Thornton JM (1993) PROCHECK: a program to check the stereochemical quality of protein structures. J Appl Cryst 26:283–291. https://doi.org/10.1107/S0021889892009944

Lee SM, Schelcher C, Demmel M et al (2013) Isolation of human hepatocytes by a two-step collagenase perfusion procedure. J Vis Exp. https://doi.org/10.3791/50615

Li L, Chen T, Stanton JD et al (2008) The peripheral benzodiazepine receptor ligand 1-(2-chlorophenyl-methylpropyl)-3-isoquinoline-carboxamide is a novel antagonist of human constitutive androstane receptor. Mol Pharmacol 74:443–453. https://doi.org/10.1124/mol.108.046656

Lindorff-Larsen K, Piana S, Palmo K et al (2010) Improved side-chain torsion potentials for the Amber ff99SB protein force field. Proteins 78:1950–1958. https://doi.org/10.1002/prot.22711

Liu ZM, Feng L, Ge GB et al (2014) A highly selective ratiometric fluorescent probe for in vitro monitoring and cellular imaging of human carboxylesterase 1. Biosens Bioelectron 57:30–35. https://doi.org/10.1016/j.bios.2014.01.049

Lynch C, Pan Y, Li L et al (2013) Identification of novel activators of constitutive androstane receptor from FDA-approved drugs by integrated computational and biological approaches. Pharm Res 30:489–501. https://doi.org/10.1007/s11095-012-0895-1

Lynch C, Zhao J, Huang R et al (2015) Quantitative high-throughput identification of drugs as modulators of human constitutive androstane receptor. Sci Rep 5:10405. https://doi.org/10.1038/srep10405

Mackowiak B, Wang H (2019) High-content analysis of constitutive androstane receptor nuclear translocation. Methods Mol Biol 1966:71–77. https://doi.org/10.1007/978-1-4939-9195-2_6

Omiecinski CJ, Coslo DM, Chen T et al (2011) Multi-species analyses of direct activators of the constitutive androstane receptor. Toxicol Sci 123:550–562. https://doi.org/10.1093/toxsci/kfr191

Piedade R, Traub S, Bitter A et al (2015) Carboxymefloquine, the major metabolite of the antimalarial drug mefloquine, induces drug-metabolizing enzyme and transporter expression by activation of pregnane X receptor. Antimicrob Agents Chemother 59:96–104. https://doi.org/10.1128/AAC.04140-14

Pissios P, Tzameli I, Kushner P, Moore DD (2000) Dynamic stabilization of nuclear receptor ligand binding domains by hormone or corepressor binding. Mol Cell 6:245–253. https://doi.org/10.1016/S1097-2765(00)00026-5

Rastinejad F, Huang P, Chandra V, Khorasanizadeh S (2013) Understanding nuclear receptor form and function using structural biology. J Mol Endocrinol 51:T1–T21. https://doi.org/10.1530/JME-13-0173

Ross J, Plummer SM, Rode A et al (2010) Human constitutive androstane receptor (CAR) and pregnane X receptor (PXR) support the hypertrophic but not the hyperplastic response to the murine nongenotoxic hepatocarcinogens phenobarbital and chlordane in vivo. Toxicol Sci 116:452–466. https://doi.org/10.1093/toxsci/kfq118

Schmidtke P, Bidon-Chanal A, Luque FJ, Barril X (2010) MDpocket: open-source cavity detection and characterization on molecular dynamics trajectories. Bioinformatics 27:3276–3285. https://doi.org/10.1093/bioinformatics/btr550

Simonsson US, Jansson B, Hai TN et al (2003) Artemisinin autoinduction is caused by involvement of cytochrome P450 2B6 but

not 2C9. Clin Pharmacol Ther 74:32–43. https://doi.org/10.1016/S0009-9236(03)00092-4

Sippl MJ (2007) Recognition of errors in three-dimensional structures of proteins. Proteins 17:355–363. https://doi.org/10.1002/prot.340170404

Tang M, Mukundan M, Yang J et al (2006) Antiplatelet agents aspirin and clopidogrel are hydrolyzed by distinct carboxylesterases, and clopidogrel is transesterificated in the presence of ethyl alcohol. J Pharmacol Exp Ther 319:1467–1476. https://doi.org/10.1124/jpet.106.110577

Tarkiainen EK, Holmberg MT, Tornio A et al (2015) carboxylesterase 1 c.428G > A single nucleotide variation increases the antiplatelet effects of clopidogrel by reducing its hydrolysis in humans. Clin Pharmacol Ther 97:650–658. https://doi.org/10.1002/cpt.101

Thasler WE, Weiss TS, Schillhorn K et al (2003) Charitable state-controlled foundation Human Tissue and Cell Research: ethic and legal aspects in the supply of surgically removed human tissue for research in the academic and commercial sector in Germany. Cell Tissue Bank 4:49–56. https://doi.org/10.1023/A:1026392429112

Theile D, Haefeli WE, Weiss J (2015) Effects of adrenolytic mitotane on drug elimination pathways assessed in vitro. Endocrine 49:842–853. https://doi.org/10.1007/s12020-014-0517-2

van Erp NP, Guchelaar HJ, Ploeger BA (2011) Mitotane has a strong and a durable inducing effect on CYP3A4 activity. Eur J Endocrinol 164:621–626. https://doi.org/10.1530/eje-10-0956

WHO (2017) WHO model list of essential medicines, 20th edition, March 2017 (amended August 2017) World Health Organization, Geneva http://www.who.int/medicines/publications/essentialmedicines/en/. Accessed 07 Dec 2018

Wilkening S, Stahl F, Bader A (2003) Comparison of primary human hepatocytes and hepatoma cell line HepG2 with regard to their biotransformation properties. Drug Metab Dispos 31:1035–1042. https://doi.org/10.1124/dmd.31.8.1035

Yan J, Chen B, Lu J, Xie W (2015) Deciphering the roles of the constitutive androstane receptor in energy metabolism. Acta Pharmacol Sin 36:62–70. https://doi.org/10.1038/aps.2014.102

Yang H, Wang H (2014) Signaling control of the constitutive androstane receptor (CAR). Protein Cell 5:113–123. https://doi.org/10.1007/s13238-013-0013-0

Zhang JH, Chung TD, Oldenburg KR (1999) A simple statistical parameter for use in evaluation and validation of high throughput screening assays. J Biomol Screen 4:67–73. https://doi.org/10.1177/108705719900400206

Zhu HJ, Wang X, Gawronski BE et al (2013) Carboxylesterase 1 as a determinant of clopidogrel metabolism and activation. J Pharmacol Exp Ther 344:665–672. https://doi.org/10.1124/jpet.112.201640